Electronic Supplementary Information for Graphene-Based Encapsulated Liquid Metal Particles

Megan A. Creighton,[a,b] Michelle C. Yuen,[a,b] Nicholas J. Morris,[a,c] and Christopher E. Tabor[a]*

[a] Air Force Research Laboratory, Materials and Manufacturing Directorate, Wright-Patterson Air Force Base, Dayton, OH, USA.
[b] National Research Council, Washington, District of Columbia 20001, USA.
[c] UES Inc., Dayton, OH, USA.
* Corresponding author email: christopher.tabor.1@us.af.mil

1 Fabrication of GO-encapsulated particles

Fig. S1 shows the procedure for producing a dispersion of GO-encapsulated eGaIn particles. First, an aqueous GO solution is prepared by bath sonicating water, a concentrated GO slurry, and pH modifier. Second, 500mg of eGaIn is added to 10mL of the aqueous solution. Third, the mixture is probe-sonicated to create the liquid metal particles, and in the process, allowing the GO sheets to self-assemble the surface of the eGaIn particles. The final schematic shows a cross-sectional view of an ideal GO-encapsulated liquid metal particle.

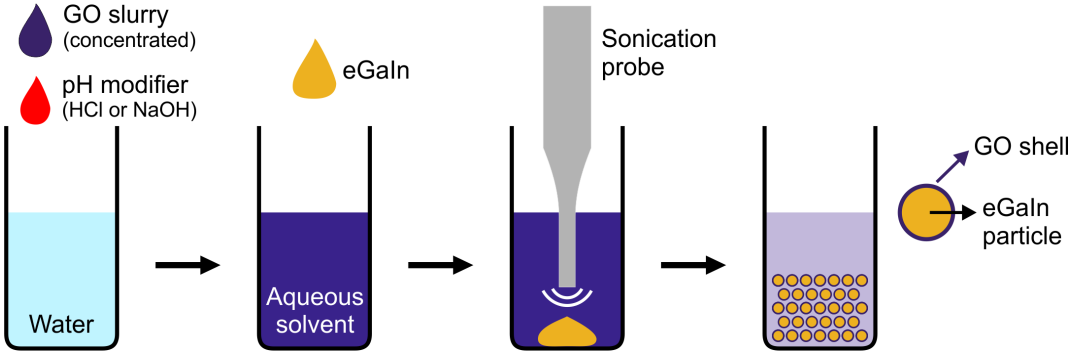

Figure S1: Fabrication sequence to produce GO-encapsulated eGaIn particles.

2 Characterization of GO and modified versions

Fig. S2 shows the FTIR data of the original GO and the two modified versions. The GO clearly has far more peaks typically associated with oxygen functionalities, such as a strong signal around 1400 for –OH bending, a broad peak around 3225 for –OH stretching, a peak at 1039 for alkoxy groups, and 1713 for carboxyl groups. The spectrum for the SHGO matches that published for the procedure used [1] and is similar to others reported in the literature. [2] It is noted that the characteristic thiol stretch at 2550 is weak and easy to overlook, however the presence of sulfur in the sample was confirmed by EDX and found to be 14%.

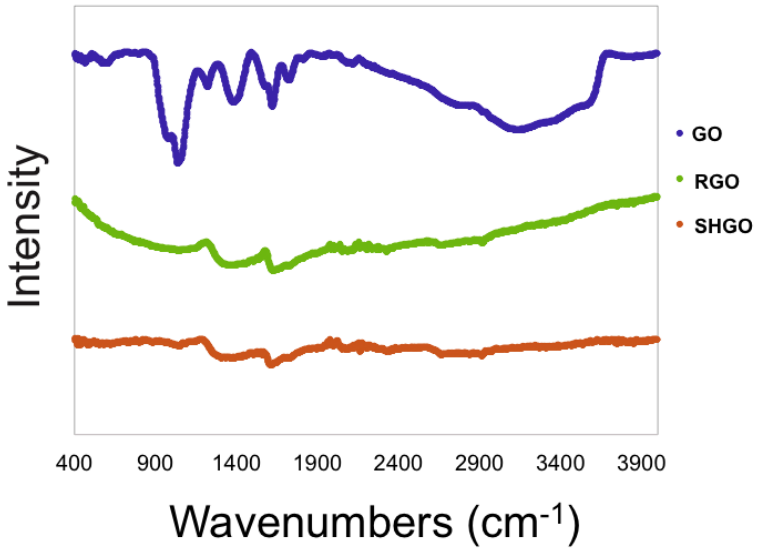

Figure S2: FTIR characterization of GO and the modified versions

3 Encapsulation by GO and modified versions using ethanol as a processing solvent

GO and the modified versions were each dispersed into vials to a final concentration of 0.5 mg/mL in 10 mL of ethanol, and bath sonicated for one hour to ensure dispersion. Then, 500 mg of eGaIn was added to each vial, and each sample was probe sonicated for 10 minutes according to the experimental procedure described in the main text. When water is used as the solvent, this is sufficient to cause GO to form a conformal encapsulating layer on the surface of dispersed liquid metal droplets. However, as can be seen in Fig. S3A in ethanol, no such encapsulation occurs. This is likely caused by the known differences in surface chemistry for the GaLMAs when processed in water vs ethanol.[3,4]. GO and its modified versions are more stable and will not incur different surface chemistries based on the solvent used. However, there could be additional subtle effects due to how the solvent molecules interact with the 2D materials. The -OH moiety in an alcohol molecule will hydrogen bond with the polar functional groups on GO, and so the ethanol molecules surrounding the 2D particle will all be oriented with their hydrophobic alkyl tails facing out in solution.[5] These alkyl tails will have no affinity for the polar functional groups on the GaLMA surface and could further impede the interaction needed for encapsulation.

The modified versions of SHGO (Fig. S3B) and RGO(Fig. S3C) also do not interact with the GaLMA surface, and show a similar surface morphology to the control sample prepared in ethanol with no 2D materials present (Fig. S3D).

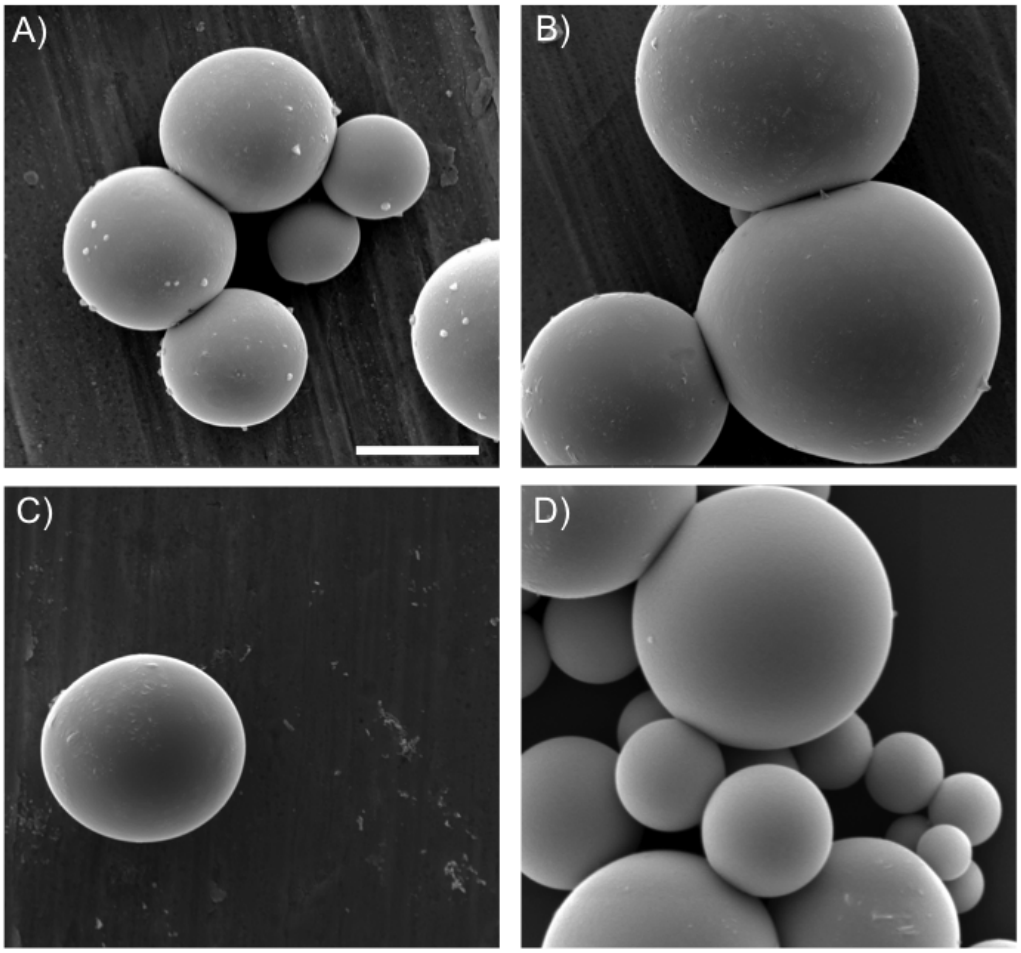

Figure S3: Encapsulation experiment carried out in ethanol in lieu of water as a processing solvent. No interaction is observed any of the A) GO B) SHGO C) RGO cases. D) Control particles of eGaIn prepared in ethanol with no 2D material present. Scalebar is 2μm.

4 GO as an antioxidant for the suppression of crystallites

In a separate study from our group, we investigate the oxidation of GaLMA surfaces, which results in the formation of gallium oxide hydroxide (GaOOH) crystallites.[4] In that work, it was found that these crystallites form very rapidly when eGaIn in sonicated in water in hypoxic conditions, due to a pathway enabled by the formation of free radicals via water sonolysis. It was also found that sodium ascorbate, a known anti-oxidant, can help suppress this pathway and delay the onset of crystallite formation. The reaction that forms GaOOH can still proceed via a slower non-radical pathway.

Graphene-family materials are also known antioxidants with a particular efficacy towards scavenging and stabilizing the hydroxyl radical.[6] They have sufficient antioxidant activity to inhibit the rapid onset of GaOOH crystallite formation in oxygen-free conditions. These results are analogous to the sodium ascorbate case presented in our other work. The graphene-family materials do not completely quench this reaction for the crystallite formation, however, as it can still proceed via the non-radical pathways. Fig. S4A shows an eGaIn LMP encapsulated in a graphene-based shell that was prepared under ambient conditions and aged in an aqueous solution overnight. The sample is covered in GaOOH crystallites, which is analogous to the observations of eGaIn LMPs that are not encapsulated with graphene oxide. It is possible that these crystallites nucleate on the LMP surface, and their growth underneath the graphene-based shell creates strain which can cause the shell to tear, as seen in Fig. S4B.

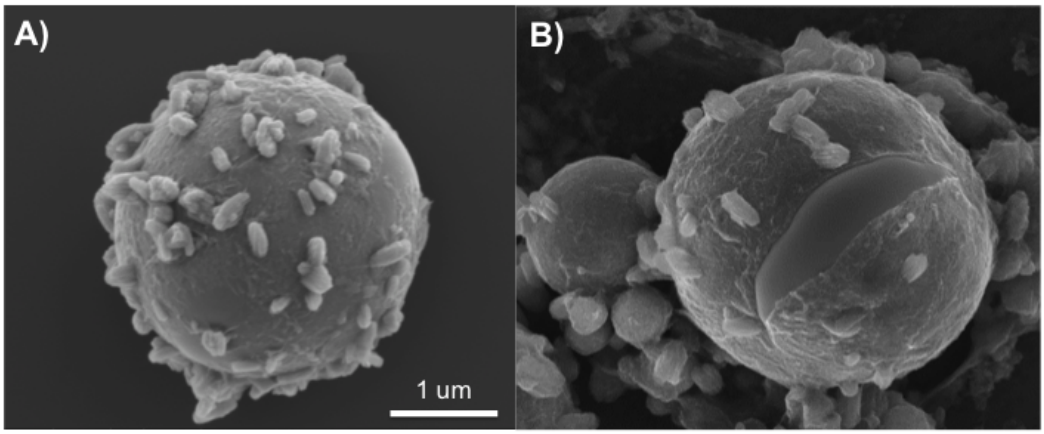

Figure S4: A) Growth of crystallites on a GO-encapsulated LMP that has been aged in water for one day. B) An enapsulated LMP whose graphene-based shell has torn and exposed the underlying liquid-metal surface.

5 XPS on GO-encapsulation of eGaIn in acidic and basic conditions

X-Ray Photoelectron Spectroscopy (XPS) measurements were performed using a Kratos Ultra XPS (Kratos, Kanagawa, Japan) with an Al K_A source having energy of 1486.69 eV. A charge compensator was used for all measurements. XPS data analysis was performed in CasaXPS software program, version 2.3.22PR1.0. Each spectrum was fitted with a background followed by fitting convoluted peaks with Gaussian–Lorentzian peaks of CasaXPS Lineshapes of GL(30). Fitting consisted of a Levenburg-Marquardt routine to minimize X^2. Samples were prepared by depositing EGaIn nanoparticle suspensions onto an Si wafer immediately after sonication and dried into films in a nitrogen environment. Samples were removed from the nitrogen environment immediately prior to loading into the XPS chamber.

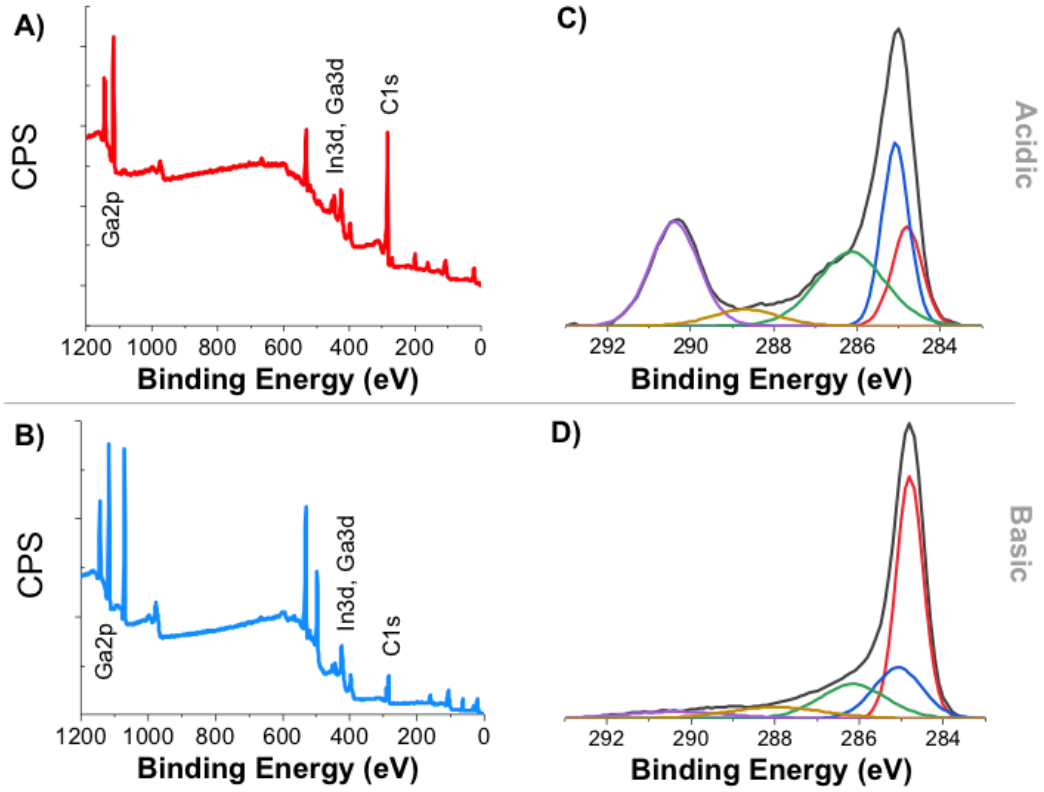

Figure S5: XPS spectra collected on GO encapsulated EGaIn LMP samples that were prepared in either acidic (0.1M HCl) or basic (0.1M NaOH) conditions. A) Survey spectrum of the sample prepared in acidic conditions. B) Survey spectrum of the sample prepared in basic conditions. C) Spectrum of the C1S region of the sample prepared in acidic conditions. D) Spectrum of the C1S region of the sample prepared in basic conditions.

The analysis shown here focuses on relative changes in the gallium, indium, and carbon signals. Samples that have been exposed to ambient conditions are known to develop a a thin layer of carbonaceous debris known as adventitious carbon, generally regarded to be only a few nanometers thick. This phenomenon is so common that the associated peak is commonly used as a reference for calibrating XPS spectra. The presence of this adventitious carbon overlaps with the signal from the GO shell, and interferes with measurements of the shell itself. However, there is qualitative support in this data about the relative thickness of the GO shell in the XPS data shown here.

The overall survey spectra (Fig. S5A,B) contain peaks from many elements, e.g. sodium and chlorine from the acid and base solutions used to adjust the pH of the solutions during manufacture of the encapsulated liquid metal particles and silicon from the underlying substrate used in preparing the samples for XPS analysis. Oxygen was also not included, because it comes from a range of sources (e.g. graphene oxide, gallium oxide, silicon oxide). The relative atomic percentages of each of these elements as determined by XPS from the survey spectra are reported in Table 1. In the acidic case, the relative amount of carbon is higher. This is congruent with a thicker GO shell. A thinner shell (i.e. from preparation in basic conditions) allows more signal from the underlying liquid metal particle, and increases the relative measured percentages of gallium and indium.

Scans were also collected for the C1S region of both samples (Fig. S5C,D). Samples that have been exposed

Table 1: Atomic composition readings of GO-encapsulated eGaIn particles by XPS.

	C	Ga	In
Prepared at acidic pH	95.3	3.6	1.1
Prepared at basic pH	86.7	11.8	1.6

to ambient conditions are known to develop a thin layer of carbonaceous debris known as adventitious carbon, generally regarded to be only a few nanometers thick. This phenomenon is so common that the associated peak (284.8 eV) is commonly used as a reference for calibrating XPS spectra. The other peaks in the spectra are the C–C (≈285.6 eV), C–O (≈286.6 eV), C=O (≈288.2 eV), and O–C=O (≈289.2 eV). Unfortunately, the presence of this adventitious carbon overlaps with the signal from the GO shell, and interferes with measurements of the shell itself. However, there is qualitative support in this data regarding the relative thickness of the GO shell in the XPS data shown here.

In the acidic case, we can observe an overall increase in the higher binding energy peaks (Fig. S5C) relative to those observed in the basic case (Fig. S5D). Higher binding energies are associated with oxidized carbon species, such as the functional groups on graphene oxide. We note note a large peak at 290.4 eV, which is not typical of graphene oxide spectra reported in the literature. A similar peak has been observed before for complexes between aluminum and carboxylic acids;[7] and we hypothesize that this peak may be the result of gallium species complexing with the carboxylic edge groups on graphene oxide platelets.

6 Particle sizing

The geometric mean radius of the GO encapsulated particles is 0.67 μm, compared to 0.55 μm for particles made in ethanol (control sample). Measurements were taken using ImageJ software. Histograms of the particle size distribution can be seen in Fig. S6.

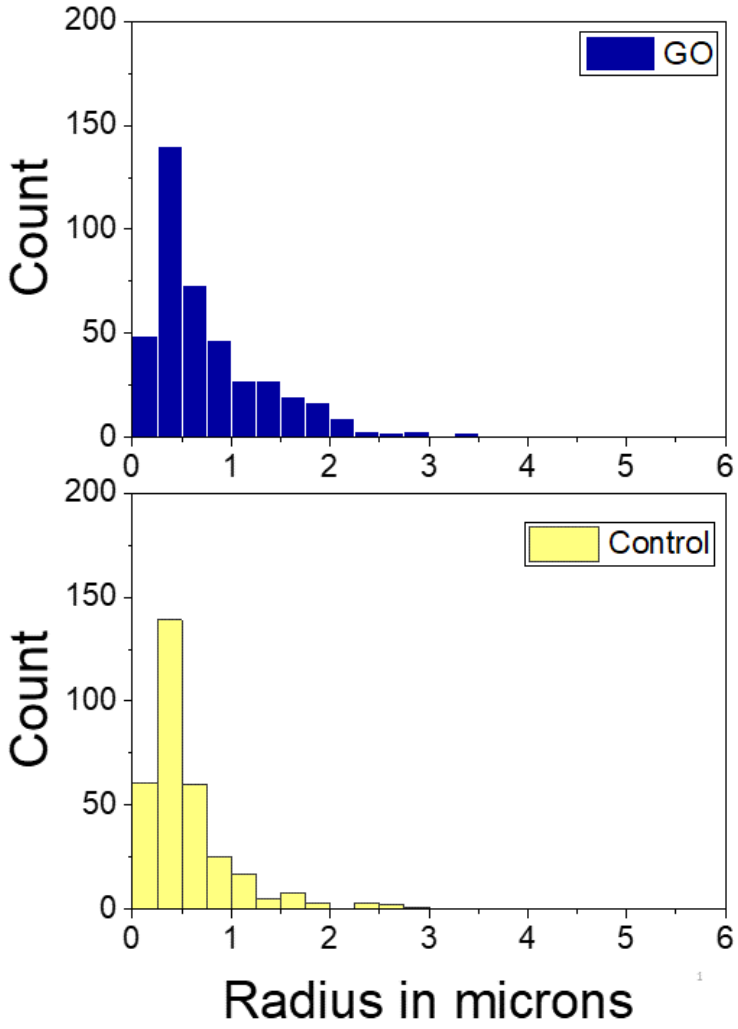

Figure S6: Histogram plot of synthesized particle radii.

7 Single particle compression

In addition to the datasets shown in the main text, several more particles were compressed (Fig. S8. The GO-encapsulated particles consistently show a prominent initial sharp load/unload peak and inelastic deformation (*i.e.*, the unloading profile does not overlap the loading profile). The unencapsulated particles, on the other hand, do exhibit a degree of elastic recovery. For particles of similar sizes, the GO-encapsulated particles have a higher initial stiffness as compared to the unfunctionalized particles, by approximately an order of magnitude. These stiffnesses were determined by using the slope of a linear fit on the load-displacement curve from the point of contact to 10% of the particle diameter. We note here though that the particles spanned a wide range of sizes which will likely affect the apparent compressive stiffness[8].

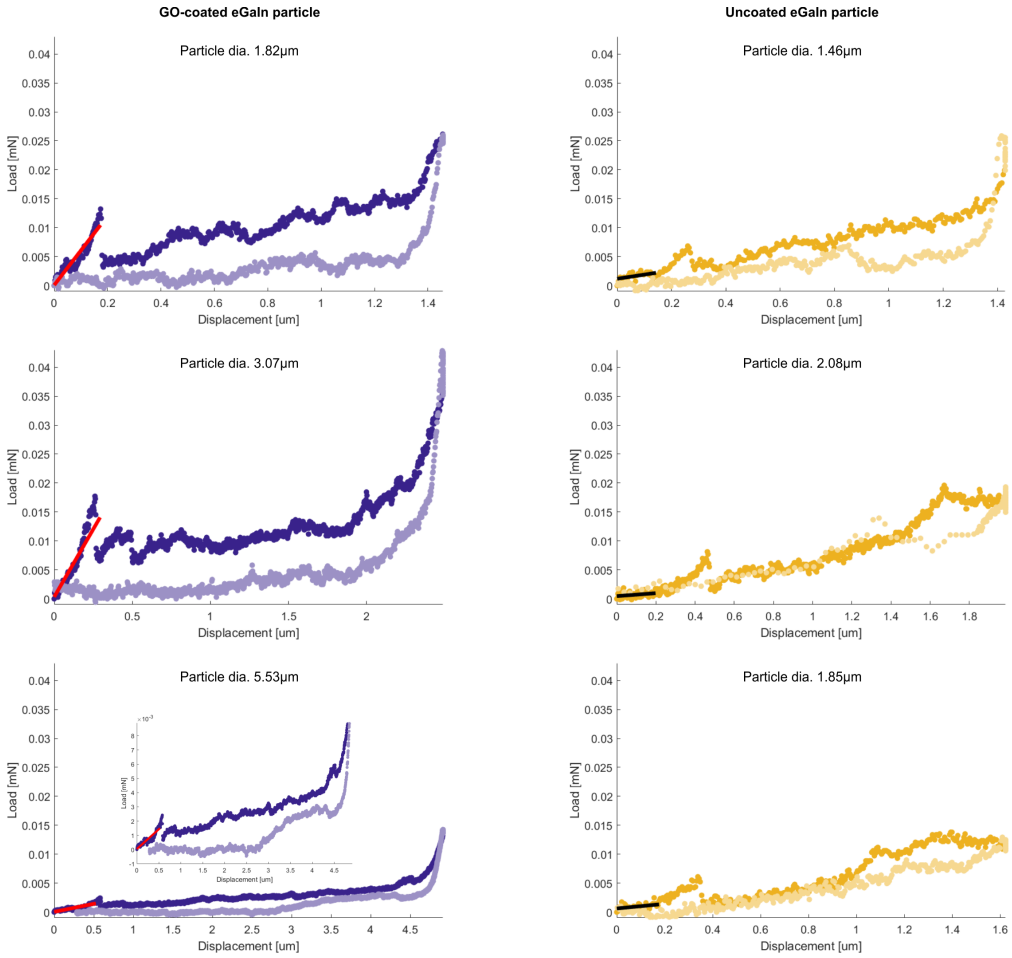

Figure S7: Load-displacement curves for single particle compression tests. The darker color shows the compressive loading phase; the lighter color is the unloading phase. The inset in the bottom left plot is a more zoomed-in view of the load-displacement curve, to better illustrate the inelastic compressive behavior of a GO-coated particle.

8 Bulk film compression

In addition to the datasets shown in the main text, bulk films comprising GO-encapsulated particles formed in acid and basic conditions were compressed (Fig. S8). The GO-encapsulated particles prepared in acidic and/or basic solutions have an initial resistance on the order of (10^5 Ω), whereas the GO-encapsulated particles prepared in neutral solution are slightly more resistive (10^6 Ω). We attribute this increase in resistance in the neutral solutions to the oxide layer that develops and contributes to the interfacial resistance between particles in the deposited ink.

As discussed above, the neutral particles exhibit a prolonged gradual decrease in resistance as greater loads are applied, followed by a relatively sharp drop in resistance before stabilizing. The acidified GO-encapsulated particles exhibit a sharp drop in resistance at much lower loads, approximately the same compressive load as the control (ethanol-sonicated) particles. In contrast, the base-sonicated GO-encapsulated EGaIn particles never exhibit a sharp change in resistance and instead the resistance decreases continuously as the compressive load increases.

We hypothesize that these differences in coalescence behavior can primarily be attributed to the number of layers in the GO encapsulating shell. Thinner GO multilayers (*i.e.* fewer layers) at the micron scale can withstand deformation to a smaller radius of curvature than thicker ones (*i.e.* more layers).[9] The GO encapsulating shell that results from the preparation in acidic conditions is the thickest, and therefore fails at the smallest loads, behaving like a brittle shell. Under neutral conditions, failure occurs at a higher load (approximately 900 N), due to a thinner GO shell (which can withstand more deformation prior to failure) and presence of gallium oxide. The electromechanical behavior of particle films prepared in basic conditions differ from all other cases and suggests a different percolation pattern. We hypothesize that this behavior is partially due to the sparse coverage of GO on these particles creating thin shells that will act like more of a membrane, allowing more 'stretching' via translation of single sheets of GO over each other, thereby dynamically encapsulating distinct droplets and hindering network formation

At the conclusion of compression, we observe smaller differences in the final resistances of the films according to ink formulation. There appears to be a trend where particles prepared in etching environments (*i.e.* acidic or basic solvents) have a lower resistance than in films prepared in neutral environments. Once dried, oxide skin may form on the EGaIn surfaces, but the oxide skin is known to mature and increase in thickness with time.[8,10] We suspect that the higher final resistance of samples prepared in neutral environments is due to impedance of coalescence by a more mature oxide skin.

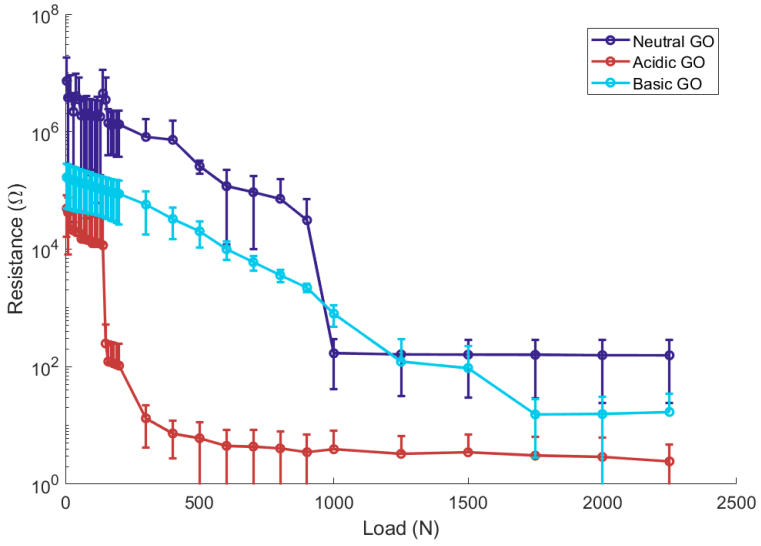

Figure S8: Resistance vs. load plots for GO-encapsulated particles formed in acidic, basic, and neutral conditions.

9 Video attachment

The video attachment shows compressions of a single GO-encapsulated eGaIn particle and an unencapsulated eGaIn particle by a 5 μm tungsten tip in a vacuum environment. Images were captured every 5 s in an SEM (FEI Quanta) and compiled in a timelapse playing at 30$\times$ speed.

References

[1] C. K. Chua and M. Pumera, *ACS nano*, 2015, **9**, 4193–4199.

[2] H. R. Thomas, A. J. Marsden, M. Walker, N. R. Wilson and J. P. Rourke, *Angewandte Chemie International Edition*, 2014, **53**, 7613–7618.

[3] M. R. Khan, C. Trlica, J.-H. So, M. Valeri and M. D. Dickey, *ACS applied materials & interfaces*, 2014, **6**, 22467–22473.

[4] M. Creighton, M. Yuen, M. Susner, B. Maruyama and C. Tabor, 2020.

[5] V. V. Neklyudov, N. R. Khafizov, I. A. Sedov and A. M. Dimiev, *Physical Chemistry Chemical Physics*, 2017, **19**, 17000–17008.

[6] G. V. Buxton, C. L. Greenstock, W. P. Helman and A. B. Ross, *Journal of physical and chemical reference data*, 1988, **17**, 513–886.

[7] P. Davies, M. Roberts and N. Shukla, *Journal of Physics: Condensed Matter*, 1991, **3**, S237.

[8] N. J. Morris, Z. J. Farrell and C. E. Tabor, *Nanoscale*, 2019, **11**, 17308–17318.

[9] D. A. Dikin, S. Stankovich, E. J. Zimney, R. D. Piner, G. H. Dommett, G. Evmenenko, S. T. Nguyen and R. S. Ruoff, *Nature*, 2007, **448**, 457–460.

[10] N. Cabrera and N. F. Mott, *Reports on progress in physics*, 1949, **12**, 163.